ARM-FIRST SYNTHESIS OF STAR POLYMERS WITH WEDGE POLYMER ARMS USING RING-OPENING METATHESIS POLYMERIZATION AND BIFUNCTIONAL CROSSLINKERS

by

Robert Learsch

S.B., Massachusetts Institute of Technology, 2015

A thesis submitted to the

Faculty of the Graduate School of the

University of Colorado in partial fulfillment

of the requirement for the degree of

Master of Science

Materials Science and Engineering Program

2017

This thesis entitled:

Arm-first synthesis of star polymers with wedge polymer arms using ring-opening metathesis polymerization and bifunctional crosslinkers

written by Robert Whitson Learsch

has been approved for the Masterials Science and Engineering Prgoram

Professor Christopher Bowman

Professor Garret Miyake

Date

The final copy of this thesis has been examined by the signatories, and we find that both the content and the form meet acceptable presentation standards of scholarly work in the above mentioned discipline.

Learsch, Robert Whitson (M. S., Materials Science and Engineering)

Arm-first synthesis of star polymers with wedge polymer arms using ring-opening metathesis polymerization and bifunctional crosslinkers

Thesis directed by Associated Professor Garret M Miyake

Recently, wedge polymers with high molecular weight, size, and rigidity have been designed and synthesized. To date, the complexity of wedge polymers has been limited to the diblock copolymer architecture. This work presents a two-step, one-pot process to make star polymers with wedge polymer arms. After the wedge polymer arms are synthesized, crosslinker species are added to the reaction, rapidly forming star polymers. Crosslinker species with different conformational freedom were designed and synthesized and their performance was evaluated. Mass conversion up to 92% and stars with up to 17 arms were synthesized with the most rigid crosslinker. The effects of arm molecular weight and molar ratio of crosslinker to arm on mass conversion and arms per star were explored further. Finally, the size scaling between the wedge homopolymer and star architectures were compared, verifying theoretical results regarding star polymers with arms much larger than their core. The positive effect of crosslinker rigidity may inform future crosslinker design.

CONTENTS

TABLES

FIGURES

CHAPTER I

INTRODUCTION

Star polymers consist of a chemically distinct core from which many (3 to 100+) polymer chains extend and form a spherical structure.[1,2] The star architecture was first accessed via anionic polymerization methods[3] and has been extensively studied as a method for affecting changes in materials properties while maintaining the chemical composition of the constituent arms.[4] To access these distinct materials properties, star polymers combine the chemical functionality of their arms with a spherical, compact shape, a high density of end-groups, and a core-shell structure similar to that of micelles.[4,5] This behavior and the relative ease of controlled synthesis lead to star polymers' popularity in sophisticated applications. Star polymers have been developed and used as additives for improving oil viscosity, biomedical devices for drug delivery, unimolecular containers for nanomaterials, and as films with improved self-assembly.[5–11]

There are three prominent strategies for star polymer synthesis: arm-first,[12,13] core-first,[8] and grafting-onto.[14,15] Arm-first synthesis aims to grow polymer arms and then crosslink them to form a core; the core-first method relies on a multi-functional initiator from which the polymer arms are grown; the grafting-onto approach reacts polymer arms with a core which have both been prepared separately. For all three methods, control over the molecular weight (MW) and chemical composition of the arms and the number of arms per star is paramount to the synthesis of star polymers that successfully execute their intended function.[9,16] For example, increases in the MW of the polymer arms leads to a transition from Newtonian to viscoelastic rheological behavior.[17] The number of arms

dictates the number of end-groups present and magnitude of star-star interactions.[18,19] Furthermore, the MW of the arms and volume fraction control the structure and dictate the microstructures accessible to the star polymer through self-assembly.[20–23] For example, star polymers with block copolymer arms can take on many morphologies inaccessible by linear block copolymers such as periodic tiling and various combinations of spheres, lamella, and cylinders.

Synthetic control of the composition and length of the polymer arms is accessible through controlled polymerization methods such as atom transfer radical polymerization (ATRP)[12] and reversible addition-fragmentation transfer (RAFT) radical polymerization,[24] or living polymerization methods such as anionic,[3] cationic,[25] ring-opening polymerization (ROP),[26] and ring-opening metathesis polymerization (ROMP).[27,28] ROMP can produce polymers with large MWs and extremely narrow molecular weight distributions (***Đ***) and is used to synthesize polymers with unique characteristics. It can also be used to synthesize designer architectures such as bottle-brush and dendritic wedge polymers.[29–35] These polymers are designed to have very high critical molecular weights and avoid chain entanglement. They act as rigid rods in solution and exhibit low glassy and plateau moduli;[34,36] this behavior is expected for polymers with low or no chain entanglement.[37,38] The distinct rigidity of bottle-brush and wedge polymers increases the critical molecular weight of the polymers, above which chain entanglement occurs. Accordingly, these types of polymers can self-assemble into morphologies with remarkably large feature sizes. Photonic crystals – nanostructures that interact with visible and infrared light – have been synthesized via self-assembly with both bottle-brush and wedge block copolymers.

Figure 1. Bottle-brush copolymer blends self-assembled to photonic crystals. Different compositions enable interactions with the full range of visible light.[39]

One way to access the bottle-brush architecture is to use macromonomers, polymer chains terminated with *exo*-norbornene, and polymerized *via* ROMP to form graft copolymers.[27,28,30,33] Recent research shows instances of ROMP being employed to synthesize star polymers from bottle-brush polymers through the arm-first approach.[27,28] In comparison, wedge polymers of the same length benefit from decreased dispersity and molecular weight due to the simplicity of their monomers.[31] However, there is no precedence for creating star polymers with wedge polymer arms. A method to reliably make star polymers from wedge polymer arms will enable the study of how star polymer behavior deviates from that of their linear counterparts.

We present the effects of crosslinker flexibility on the formation of star polymers using the arm first approach. The flexibility-performance relationship observed across the crosslinkers may inform future crosslinker design. The star polymers formed throughout this study are unique due to the high rigidity, length, and MW of the wedge polymer arms. We find trends relating arm MW and crosslinker ratio to arm conversion and arms per star. Finally, we experimentally verify the scaling relationship of size and MW for the linear and star polymers predicted from a previous theoretical analysis.[40–42]

CHAPTER II

MATERIALS AND METHODS

All chemicals were purchased from Sigma-Aldrich or VWR, unless otherwise reported. All polymerizations were carried out inside a nitrogen filled glovebox.

*ROMP catalyst (**1**) ($(H_2IMes)(py)_2(Cl)_2RuCHPh$).* $(H_2IMes)(PPh_3)(Cl)_2RuCHPh$ was received as a research gift from Materia Inc. and was converted to $(H_2IMes)(py)_2(Cl)_2RuCHPh$ (**1**) via literature procedure.[43]

1,10-di-norbornene decane (R_A). 2.2 equivalents of cis-5-Norbornene-exo-2,3-dicarboxylic anhydride (exo-norbornene) (500 mg, 3.05 mmol) and 1 equivalent of 1,10-diaminodecane (240 mg, 1.39 mmol), neat, were stirred at 140 ˚C in a sealed, thick-walled glass flask for 60 minutes. After the reaction cooled, the mixture was dissolved in CH_2Cl_2 and filtered through a plug of silica. The resulting product was dried by rotary evaporation and crystallized from diethyl ether. The crystals were isolated by filtration and dried overnight *in vacuo*. Yield 20% (129 mg). ^{1}H NMR (300 MHz, $CDCl_3$) δ 6.23 (t, J = 1.9 Hz, 4H), 3.45 – 3.33 (m, 4H), 3.22 (p, J = 1.7 Hz, 4H), 2.62 (d, J = 1.4 Hz, 4H), 1.55 – 1.39 (m, 6H), 1.31 – 1.08 (m, 15H). ^{13}C (75 MHz, $CDCl_3$) δ 178.1, 137.9, 47.82, 45.19, 44.93, 42.75, 38.75, 29.33, 29.09, 27.78, 26.95.

Para-xylene dinorbornene (R_B). A 100mL thick-walled flash was equipped with a stir bar and flame-dried under vacuum. Once cooled, the flask was back filled with nitrogen 2.2 equivalents of cis-5-Norbornene-exo-2,3-dicarboxylic anhydride (exo-norbornene) (500 mg, 3.05 mmol) and 1 equivalent of para-xylenediamine (189 mg, 1.39 mmol) were

added. 10 mL of DMF, obtained from a MBRAUN solvent system, was added without further treatment and the reaction was stirred at reflux (160 ˚C) overnight. Overnight, a white solid formed and settled to the bottom of the DMF solution. The solid was separated by filtration and dried *in vacuo*. Yield 60% (357 mg). ^{1}H NMR (300 MHz, $CDCl_3$) 7.30 (s, 4H), 6.27 (t, J = 1.9 Hz, 4H), 3.24 (p, J = 1.7 Hz, 4H), 2.67 (d, J = 1.4 Hz, 4H), 1.40 (dt, J = 9.9, 1.6 Hz, 2H), 1.03 (ddt, J = 10.0, 1.6, 0.9 Hz, 2H). ^{13}C NMR (75 MHz, $CDCl_3$) δ 177.8, 138.1, 135.7, 129.3, 47.96, 45.44, 42.81, 42.12.

Para-phenylene dinorbornene (R_C). A 100mL thick-walled flash was equipped with a stir bar and flame-dried under vacuum. Once cooled, the flask was back filled with nitrogen and 2.2 equivalents of cis-5-Norbornene-exo-2,3-dicarboxylic anhydride (exo-norbornene) (500 mg, 3.05 mmol) and 1 equivalent of para-phenylenediamine (150 mg, 1.39 mmol) were added. 10 mL of DMF, obtained from a MBRAUN solvent system, was added without further treatment and the reaction was stirred at reflux (160 ˚C) overnight. Overnight, a white solid formed and settled to the bottom of the DMF solution. The solid was separated by filtration and dried to pearlescent flakes *in vacuo*. Yield 63% (345 mg). ^{1}H NMR (300 MHz, $CDCl_3$) δ 7.42 (s, 4H), 6.35 (t, J = 1.9 Hz, 4H), 3.41 (p, J = 1.8 Hz, 4H), 2.86 (d, J = 1.3 Hz, 4H), 1.62 (dt, J = 9.9, 1.6 Hz, 2H), 1.45 (dt, J = 9.9, 1.5 Hz, 2H). ^{13}C NMR (75 MHz, $CDCl_3$) δ 176.8, 138.2, 131.9, 127.0, 77.58, 77.16, 76.74, 48.02, 46.05, 43.16.

Benzyl Wedge. Benzyl wedge monomer (BnW) was prepared via literature procedure.[31]

Poly(BnW). Poly(BnW) was prepared via literature procedure.[31] One hour after the addition of catalyst, the concentration of BnW was adjusted to facilitate precise and convenient aliquots for the star polymer synthesis.

Star(Poly(BnW)). The desired amount of crosslinker was dissolved with 4mL DCM in a 20 mL vial with a poly(ethylene) lining on the cap and stirred vigorously. One hour after the initial addition of catalyst, 1 mL aliquots from the polymer solution were added rapidly to the vigorously stirring solution. After 2, 6, or 24 hours, the reaction was quenched by the addition of 150 μL of ethyl vinyl ether. Star polymers were isolated by drying the mixture to a saturated solution, precipitating with methanol (MeOH), and filtering and washing the resulting solid with MeOH. The star polymer products were dried in a vacuum oven at 50 ˚C overnight.

Gel permeation chromatography with multi-angle light scattering (GPC-MALS). Polymer molecular weights were determined by gel permeation chromatography (GPC) coupled with multiangle light-scattering (MALS), using an Agilent HPLC fitted with one PLgel 5 μm guard column and three PLgel 5 μm MIXED-C gel permeation columns, a Wyatt Technology TrEX differential refractometer, and a Wyatt Technology miniDAWN TREOS light scattering detector, using THF as the eluent at a flow rate of 1.0 mL/min. Absolute molecular weights were determined using *d*n/*d*c values calculated by assuming 100% mass recovery of the polymer sample with a known concentration injection onto the GPC. The *d*n/*d*c of poly(BnW) = .1702, *dn/dc* of star(poly(BnW)) = .2116 was determined using the *d*n/*d*c of isolated arms and assuming 100% mass recovery.

Nuclear Magnetic Resonance (NMR) characterization. NMR spectra were recorded on Bruker 300 MHz spectrometer ($^{1}H/^{13}C$). Chemical shifts were referenced to internal solvent resonances using $CDCl_3$ (^{1}H: 7.26 ppm; ^{13}C: 77.16 ppm) and are reported as parts per million relative to tetramethylsilane.

CHAPTER III

RESULTS AND DISCUSSION

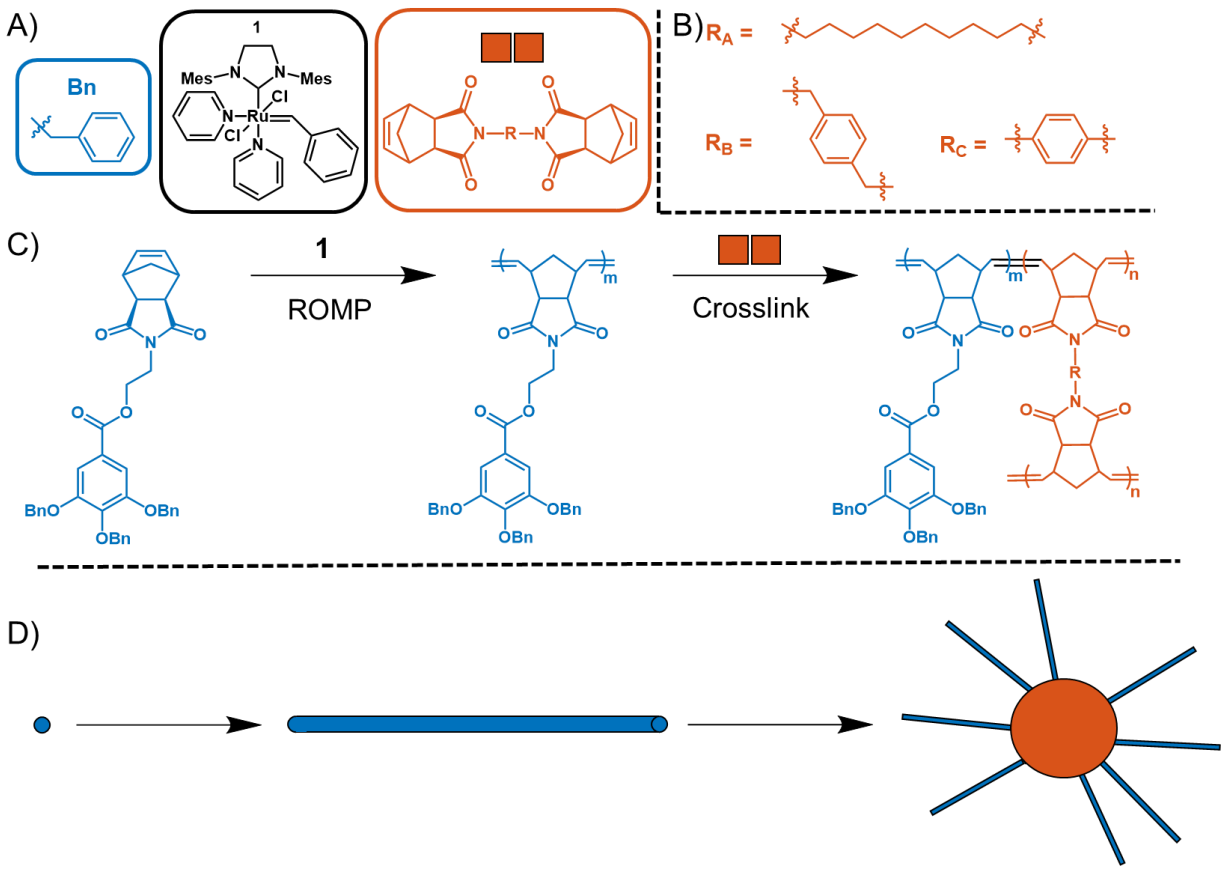

Figure 2. A) Structure of the benzyl wedge monomer (BnW), ROMP catalyst (**1)** (Mes = mesitylene), and a generic crosslinker. B) Chemical core of the different crosslinkers investigated in this study. C) Reaction scheme for synthesis of homo(BnW) and star(homo(BnW)) from BnW monomer D) A schematic of the synthetic approach and the resulting polymer.

Crosslinker Comparison. As crosslinker flexibility was hypothesized to influence the efficiency of star formation, three crosslinkers were designed with varying levels of flexibility between the anhydrous cis-5-Norbornene-exo-2,3-dicarboxylic anhydride (*exo*-norbornene groups. By reacting decane (R_A), para-xylene (R_B), and para-phenylene (R_C)

diamines with *exo*-norbornene, three di-functional compounds were synthesized and investigated as crosslinkers (Figure 2 B). The R_A crosslinker is composed of nine C-C single bonds that impart a high degree of conformational freedom between the exo-norbornene functionalities. In comparison, the R_C crosslinker is rigid, with only a phenyl ring connecting the norbornene groups. To test the capacity of the crosslinkers to form star polymers, homo(benzyl wedge) (BnW) was synthesized via ROMP and crosslinker was added *in-situ*. The resulting products were analyzed by gel permeation chromatography (GPC) coupled with multi-angle light scattering (MALS) (Table 1)**.** Across a wide range of molecular weights and through variation of the ratio of crosslinker to polymer, the R_C crosslinker consistently achieved the highest star weight-average molecular weight (M_w) and mass conversion. The R_A crosslinker failed to achieve higher than 10% mass conversion and forms mostly dimeric species.

TABLE 1. Summary of star polymer synthesis using R_A, R_B, and R_C crosslinkers.

R_A							
Arm M_W (kDa)[a]	Arm $Đ$ (M_w/M_n)	[R_A]:[**1**][b]	Star M_W (kDa) [a]	Star $Đ$ (M_w/M_n)	Mass conv. (%)[a]	# of arms[c]	R_n (nm)[d]
57.8	1.01	5.8	111	1.02	2.0	1.9	7.2
57.8	1.01	23	123	1.02	5.7	2.0	9.1
133	1.02	6.7	207	1.02	1.9	1.5	13
133	1.02	27	230	1.02	3.8	1.6	14
232	1.01	5.4	395	1.06	0.5	1.7	19
232	1.01	22	412	1.01	1.4	1.7	21
R_B							
Arm M_W (kDa)[a]	Arm $Đ$ (M_w/M_n)	[R_B]:[**1**][b]	Star M_W (kDa) [a]	Star $Đ$ (M_w/M_n)	Mass conv. (%)[a]	# of arms[c]	R_n (nm)[d]
28.8	1.01	7.1	62.3	1.08	53	2.1	-
28.8	1.01	28	94.3	1.10	68	2.9	3.0
40.0	1.01	13	68.8	1.17	43	1.7	-
40.0	1.01	25	90.3	1.07	52	2.3	4.4
40.0	1.01	50	100	1.08	59	2.5	5.6
101	1.00	10	180	1.05	22	1.8	11
101	1.00	20	201	1.05	27	2.0	11

101	1.00	34	216	1.07	30	2.1	11
124	1.01	7.0	225	1.02	18	2.6	14
124	1.01	28	258	1.05	32	2.9	13
R_C							
Arm M_W (kDa)[a]	Arm $Đ$ (M_w/M_n)	[R_C]:[**1**][b]	Star M_W (kDa) [a]	Star $Đ$ (M_w/M_n)	Mass conv. (%)[a]	# of arms[c]	R_n (nm)[d]
28.8	1.01	7.1	137	1.14	82	4.6	4.0
28.8	1.01	28	341	1.11	92	11	6.9
40.0	1.01	25	154	1.13	76	3.9	6.3
40.0	1.01	50	249	1.07	81	6.2	7.3
101	1.01	10	562	1.09	59	5.6	15
101	1.01	20	870	1.09	76	8.6	17
101	1.01	40	1090	1.07	89	11	16
124	1.01	7.0	336	1.09	39	2.7	17

[a] Determined by gel permeation chromatography. [b] Assumes 100% conversion from BnW monomer to homo(BnW). [c] Determined by light scattering, adjusted to account for the added mass of the crosslinker. [d] Determined by multi angle light scattering.

The GPC-MALS analysis reveals the non-equivalent ability of each crosslinker to produce star polymers (Figure 3). When the most flexible crosslinker, R_A, is added, the star polymer product peak has a low intensity; only 5.7% of the polymer arms are converted to two-arm products. Using the crosslinker with intermediate flexibility, R_B, in a similar reaction results in 52% of the polymer arms converting to star polymers with two to three arms. When the most rigid crosslinker, R_C, is used, 76% of the polymer arms react to form star polymers with four arms. As shown in Table 1, for all M_w and ratios of crosslinker to arms, the star polymers produced from the R_C crosslinker has higher M_W than the products from either the R_A or R_B crosslinker reactions. The R_C crosslinker is the most effective at forming star polymers with high conversion and with many arms per star.

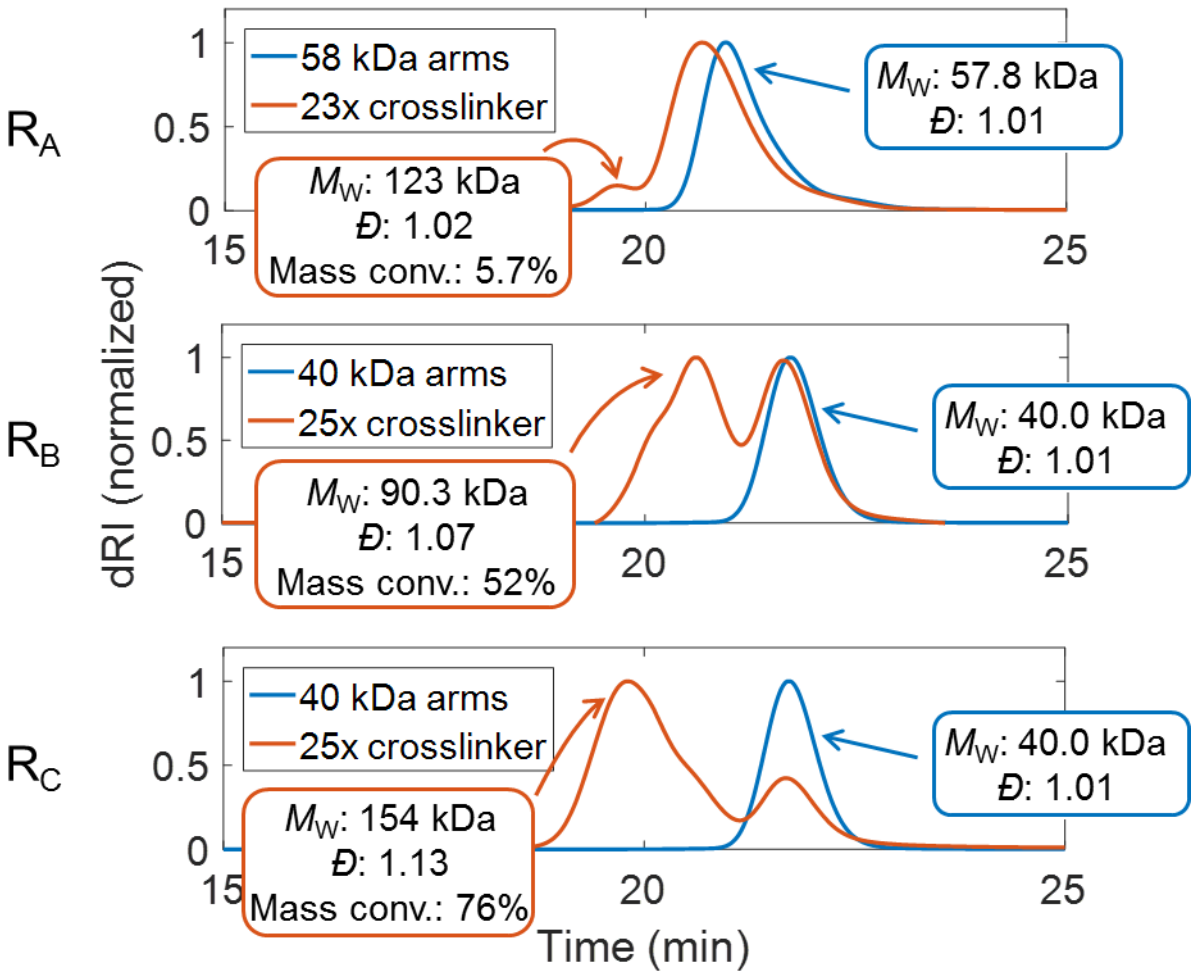

Figure 3. GPC traces for star polymers produced by reacting similar molar ratios of R_A, R_B, and R_C crosslinkers with homo(BnW) wedge polymers of similar molecular weights. The red traces were taken after the reaction proceeded for 2 hours after addition of crosslinker.

Upon addition to the polymerization solution, the crosslinkers react with the catalyst (**1**) on the end of polymer arms. These arm-crosslinker species continue to polymerize with the excess crosslinkers and polymer arms in solution. Because the crosslinkers are di-functional, there is an unpolymerized *exo*-norbornene group for each polymerized crosslinker molecule. The unpolymerized *exo*-norbornenes can further react with the homo(BnW) arms or additional arm-crosslinker compounds in the polymerization solution.

When low-MW (degree of polymerization (DP) < 150) arms are reacted with any of the crosslinkers, complete polymerization of both *exo*-norbornene functionalities on the crosslinkers is observed through the disappearance of norbornene double bonds by NMR analysis of the star polymers (Figure 4).

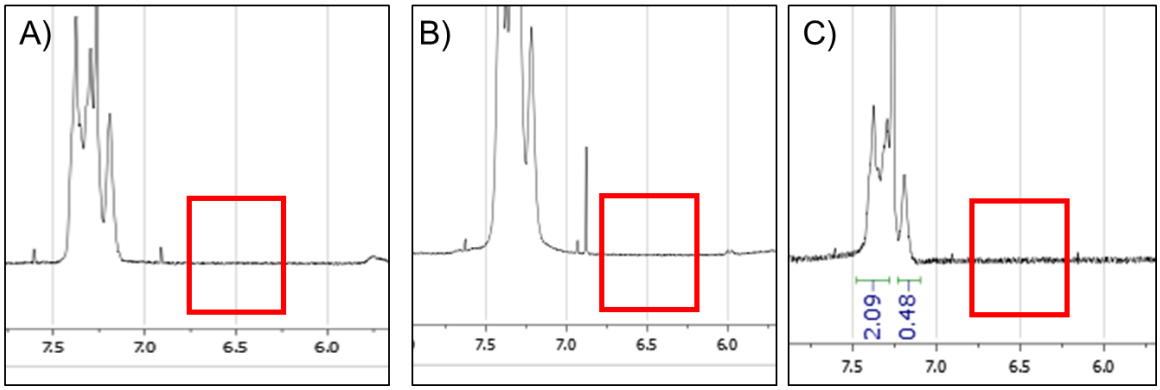

Figure 4. ^{1}H NMR ($CDCl_3$) spectra of various star polymer products. A) 1,10-Dinorbornene decane reacted with 58 kDa polymer arms. B) Para-xylenedinorbornene reacted with 29 kDa polymer arms and C) Para-phenylenedinorbornene reacted with 518 kDa polymer arms. The highlighted area shows the absence of an unreacted double bond in the norbornene groups.

Through this process, all the crosslinkers added to the reaction mixture are incorporated into the star polymer to form the core. The *exo*-norbornene functionalities have polymerized with either additional crosslinkers or polymer arms. Despite the complete polymerization of crosslinker in the product, each crosslinker tested produced incomplete conversion to star polymers, shown by the presence of the arm peak on GPC. Once all the crosslinker in solution has been incorporated into the core, a pathway arises to cease polymerization and explain these two observations. If an *exo*-norbornene across from the chain reacts with an active site on the end of a chain, it will polymerize without adding additional arms or crosslinkers to the chain. Once this intramolecular

polymerization occurs, there will be no remaining unreacted norbornene functionalities, preventing new polymer arms or polymer arm-crosslinker compounds from binding to the star polymer. Crosslinker flexibility increases the likelihood of the intramolecular polymerization events that prevent the further formation of star polymers.

Additionally, for high-MW (DP > 150) arms reacted with the R_B and R_C crosslinkers, there are no unpolymerized crosslinker present by NMR analysis. The R_A crosslinker, however, presents an exception. When the R_A crosslinker was reacted with 58 kDa arms, every *exo*-norbornene group polymerized and participated in the reaction. In comparison, when reacted with 133 kDa arms, approximately 28% of the *exo*-norbornene groups remained unpolymerized (Figure 5).

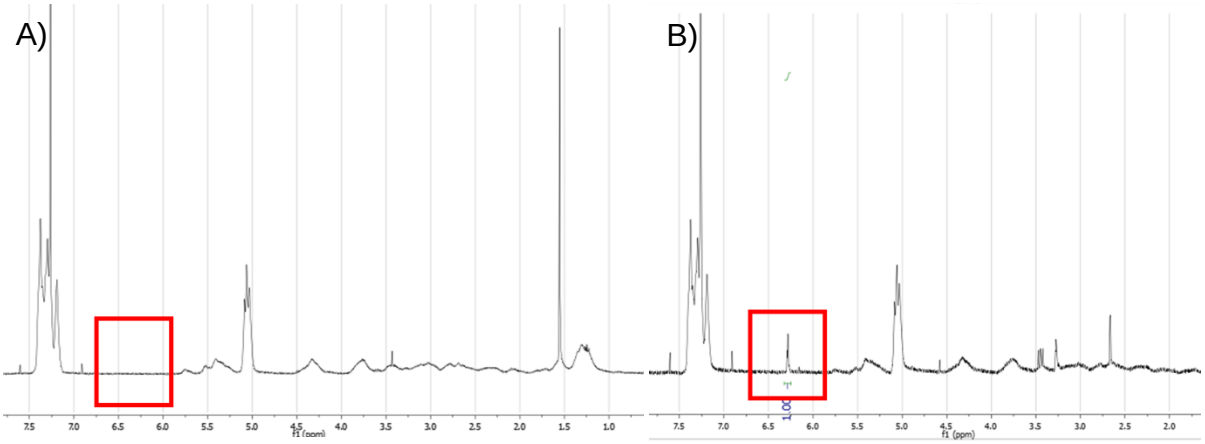

Figure 5: A) ^{1}H NMR ($CDCl_3$) of star polymer product formed from reacting RA with 58 kDa polymer arms. B) ^{1}H NMR ($CDCl_3$) of star polymer product formed from reacting R_A with 133 kDa arms.

This is due to a combination of two factors: the flexibility of the crosslinker and the increased steric bulk of the high MW polymer arms. The rapid addition of decane-containing crosslinkers to the polymer chains creates a high local concentration of flexible chains. Some of these chains become entangled within the core,[44] creating trapped *exo*-

norbornene groups inside the core. These groups are rendered inaccessible to additional polymer arms by a combination of trapped end groups and bulky arms, preventing further arms from reacting with the available *exo*-norbornene functionalities. The steric hindrance in the system results in norbornene groups that stay unpolymerized but react extremely slowly or not at all, which is observed via GPC (Figure 3).

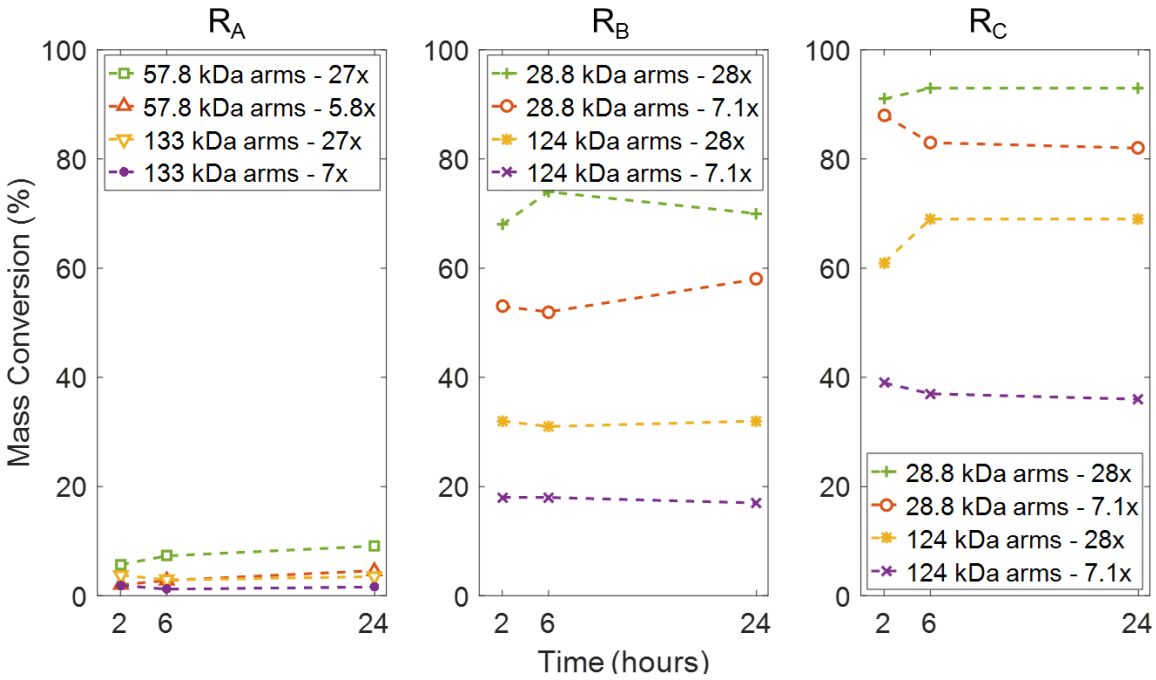

Figure 6. Plots of mass conversion as a function of time for homo(BnW) polymers reacted with R_A, R_B, and R_C crosslinkers with similar polymer arm M_W and crosslinker concentrations after 2, 6, and 24 hours. The legend states the M_W of the polymer arm and the molar equivalents of crosslinker used.

To further test the hypothesis that crosslinker flexibility hinders star formation and arm incorporation, a reaction of each crosslinker with various polymer MW and crosslinker ratios was monitored for 24 hours. Analysis by GPC-MALS reveals that regardless of the polymer MW or the amount of crosslinker, the reaction typically proceeds at a dramatically slower or rate (R_A) or ceases to proceed (R_B and R_C) within 2 hours of crosslinker addition (Figure 6). This result confirms that the available norbornene species react rapidly when

added to the polymer solution. The rapid reaction of *exo*-norbornene functionalities on the crosslinkers ultimately leads to intra-core polymerization events, ending the growth of individual macromolecules. A crosslinker that can rotate freely - such as R_A - is more likely to participate in intramolecular polymerization, rapidly ceasing polymerization, and producing star polymers in lower yield.

Effect of polymer arm molecular weight. Illustrated in Figure 6 and Table 1, the molecular weight of the polymer arms has a pronounced effect on the ability of any crosslinker to produce star polymers. The mass conversion of polymer arms to star polymers decreases as polymer arm MW increases. A similar result is observed as the molar amount of crosslinker decreases. To investigate these dependencies, the R_C crosslinker, which preliminary testing determined to give the highest conversion, was reacted with homo(BnW) arms over a wide range of MW and crosslinker ratios. Aliquots from a polymerization solution with active catalyst were added to vials of crosslinker solutions at different concentrations. This process assessed the formation of stars from a wide range of polymer arm M_w (from 101 kDa to 805 kDa) and molar ratios of crosslinker to polymer arm (from 10 to 233) (Figure 7 and Table 2**)**.

TABLE 2. Summary of star polymer synthesis using R_C crosslinker.

R_C							
Arm M_W (kDa)[a]	Arm $Đ$ (M_W/M_n)	[R_C]:[**1**][b]	Star M_W (kDa) [a]	Star $Đ$ (M_W/M_n)	Mass conv. (%)[a]	# of arms[c]	R_n (nm)[d]
28.8	1.01	7.1	137	1.14	82	4.6	4.0
28.8	1.01	28	341	1.11	92	11	6.9
40.0	1.01	25	154	1.13	76	3.9	6.3
40.0	1.01	50	249	1.07	81	6.2	7.3
101	1.01	10	562	1.09	59	5.6	15
101	1.01	20	870	1.09	76	8.6	17
101	1.01	40	1090	1.07	89	11	16
101	1.01	85	1740	1.07	92	17	18

124	1.01	7.0	336	1.09	39	2.7	17
124	1.01	28	488	1.05	63	3.8	15
225	1.03	11	1080	1.12	52	4.7	23
225	1.03	22	1350	1.10	65	5.9	25
225	1.03	57	1820	1.10	64	7.9	27
225	1.03	91	2510	1.08	79	11	28
527	1.07	13	1850	1.08	45	3.6	38
527	1.07	26	1900	1.08	51	3.6	37
527	1.07	65	3410	1.04	61	6.5	43
527	1.07	104	3300	1.05	63	6.3	42
527	1.07	233	5210	1.01	71	9.9	43
805	1.01	13	1780	1.05	27	2.2	48
805	1.01	27	2340	1.08	41	2.9	51
805	1.01	54	3860	1.05	45	4.8	59
805	1.01	107	5350	1.00	55	6.5	62
805	1.01	215	6900	1.00	61	8.5	62

[a] Determined by gel permeation chromatography. [b] Assumes 100% conversion from BnW monomer to homo(BnW). [c] Determined by light scattering, adjusted to account for the added mass of the crosslinker. [d] Determined by multi angle light scattering.

GPC analysis shows that both mass conversion and the number of arms per star increased logarithmically as the molar equivalents of crosslinker is increased. The logarithmic response plateaued more quickly for polymer arms with higher MW.

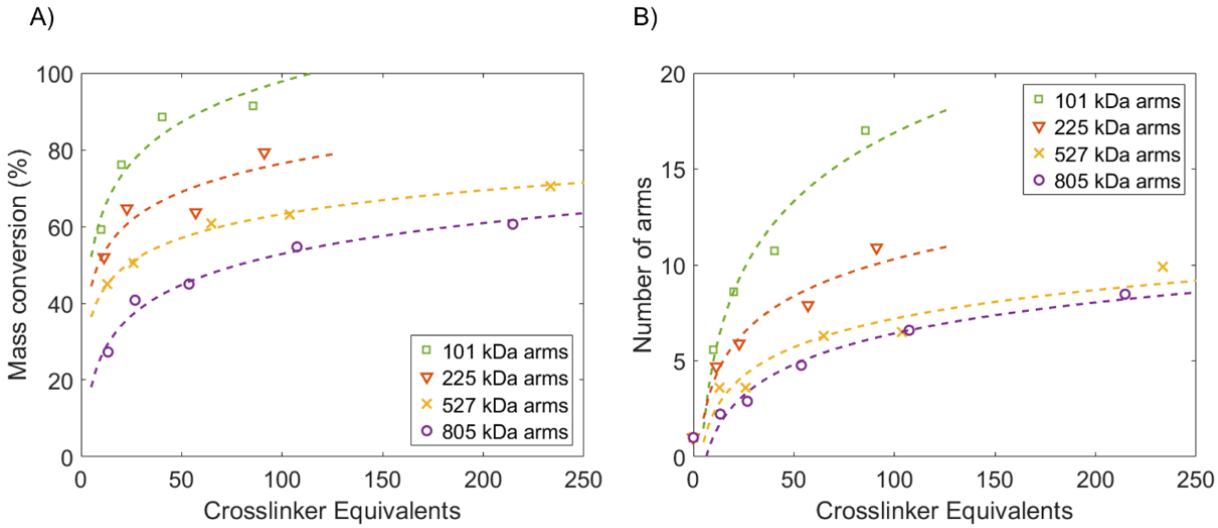

Figure 7. Plots of A) mass conversion and B) number of arms incorporated as a function of molar equivalence of R_C crosslinker added. The open markers show the data points; the dashed lines show a logarithmic fit.

It is worth noting that these two metrics could be independent. For example, a possible outcome of adding more crosslinker could be to form more dimers, increasing mass conversion but not arms per star. However, in this system, the mass conversion and number of arms follow the same trend: as the conversion increases, there are both fewer unreacted arms and more arms per star. This behavior is revealed by GPC traces of polymer products formed by reacting the same homo(BnW) arms with various ratios of crosslinker. The increase in crosslinker equivalents simultaneously reduces the intensity of the arm peak and cause the product to elute earlier, showing a star with higher MW and more arms.

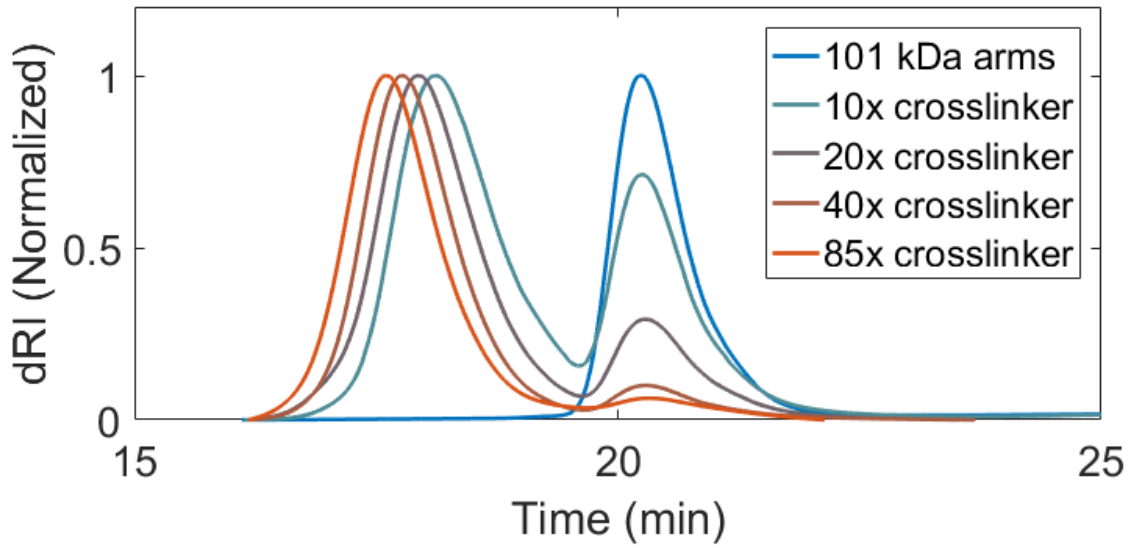

Figure 8. Overlaid GPC traces of the 101 kDa arms (green curve, Figure 4) reacted with different molar amounts of the R_C crosslinker. All product traces were collected two hours after the crosslinker was added.

Decrease in conversion and arms per star is a direct result of the increase in MW of the polymer arms. Recent research on star polymers has reported the poor ability of arms with a large DP to form star polymers with high conversion and many arms per star.

[12] Specifically, a marked decrease in mass conversion as the DP of a polymer arm exceeded 150 is noted. The polymer arms in the present study (Figure 7) had DPs ranging from 171 (101 kDa, green) to 1370 (805 kDa, purple) and the conversion-diminishing effect (92% to 55% conversion, at a crosslinker ratio of 85:1) of MW was pronounced within that range. The previous study fixed crosslinker equivalents at 14, so to the best of our knowledge there are no previous results for star polymers formed from high DP arms with the high crosslinker equivalents used here. We suspect the same phenomena cited previously are responsible for the behavior observed here: long polymer chains have lower mobility and sterically hinder the incorporation of additional arms. Increased chain length lowers the rate at which polymer arms attach to the core, biasing the core composition further toward crosslinker-crosslinker bonds. The steric bulk of the large polymer arms obstruct the incorporation of successive arms, resulting in lower mass conversion and fewer arms per star. As shown in this work, an increase in crosslinker equivalents results in increased star polymer yield and higher DP arms require more crosslinker to reach the same yields obtained with lower DP arms.

Conformation of polymer arms and product in solution. A polymer's conformation in solution can be elucidated from how a change in molecular weight changes the polymer's size. These two metrics are related by the scaling exponent, determined by plotting M_W against radius. This analysis is shown for both the homo(BnW) polymer arms (Figure 9 A) and the star polymer products (Figure 9 B).

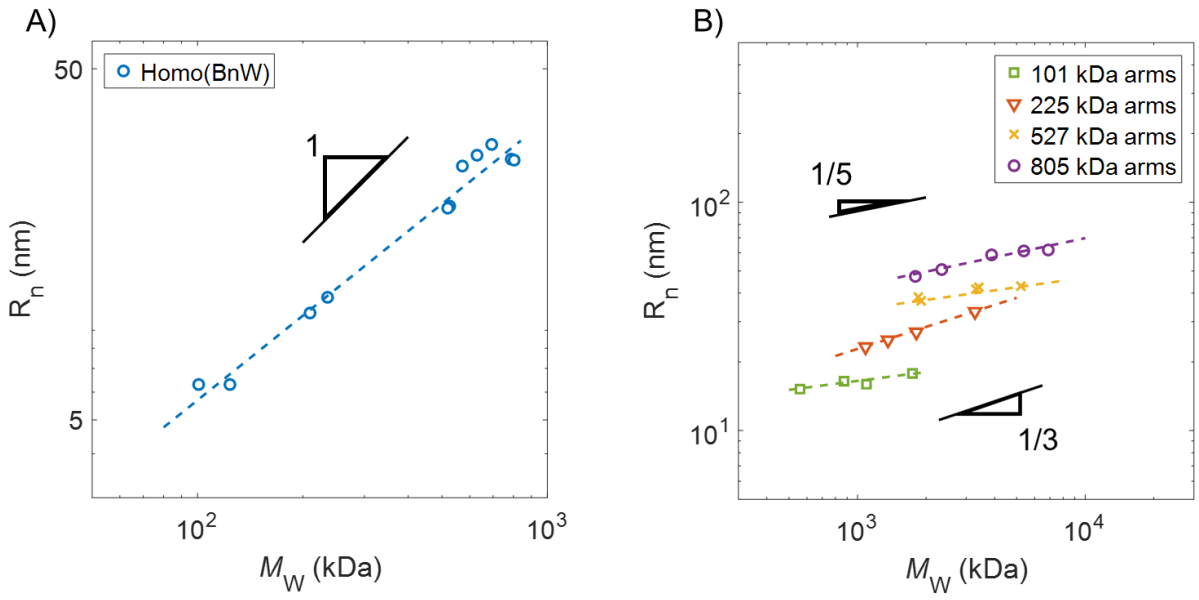

Figure 9. A) Log-log plots of homo(benzyl wedge) M_W series against the number average radius, R_n. The markers represent experimental data; the dashed line represents the power fit. The slope of the fitted lines, which reveals the molecular conformation in solution, is .90 for the homo(benzyl wedge). The guideline drawn (black) is for ideal rigid-rod polymers (slope = 1). B) Log-log plots of the M_w against number average radius for the linked product produced by reacting with the phenylene based crosslinker with arms of different molecular weights. The markers represent experimental data; the dashed line represents the power fit. The calculated slopes are .13 (101 kDa arms, green), .32 (225 kDa arms, red), .14 (527 kDa arms, yellow), and .21 (805 kDa arms, purple). The guidelines drawn are for hard-sphere polymers (slope = 1/3) and star polymers with a small number of very long arms (slope = 1/5).[40]

A polymer which behaves like an ideal rigid rod in solution would only expand in one dimension as mass is added. Accordingly, a rigid rod would have a scaling exponent of 1.0. The BnW monomer was designed to polymerize into a rigid rod and discourage chain entanglement.[31,32] The analysis relating M_w and R_n shows the polymer arms coil very little in solution; instead they rapidly gain length as weight is added. These results show the scaling exponent for the homo(BnW) to be .90 (R^2 = .83).

For the star polymers, the same analysis reveals scaling exponents that are much lower; the star polymer size increases very slowly as mass is added. Theoretical results

predict that the scaling exponent for star polymers in a good solvent to be 1/5.[40] This prediction only holds for star polymers where the arms are very long and the number of arms is small, which is a regime into which all star polymers in this study fall. To our knowledge, this work is the first experimental result directly verifying these predictions for polymers with few (< 20) arms.[17] The experimentally measured values for these exponents range from .13 and .32, which are lower than the predicted scaling exponent for a hard sphere (1/3), but in line with the results predicted by theory (1/5).

The radius of the star polymer is dictated by the length of the arms, not directly by the M_W of the star polymer. For example, doubling the number of arms from 4 to 8 dramatically changes the density of the star polymer, but not the volume. To explain the slight increase in radius, the role solvent plays in conformation must be considered. THF is a good solvent for these polymers; the monomers thermodynamically prefer to be surrounded by solvent over other monomer units. As the star polymer incorporates more arms, the area near the core becomes congested and those repeat units near the center are brought closer to other polymer chains. Consequently, the arms expand further to maximize their contact with the solvent. The extension of the arms as more are added causes the slight radius increase seen as a function of star polymer MW. As the individual arms are nearly fully extended before they are incorporated into the star, the potential for increase in radius is small.

CHAPTER IV

CONCLUSIONS

Several bifunctional crosslinkers have been synthesized and used to synthesize star polymers from wedge polymer arms. The most rigid crosslinker was determined to provide the highest conversion and arms per star across a wide range of high polymer arm MWs. A logarithmic response in conversion and arm incorporation was observed as the ratio of crosslinker to arms was increased. Increasing polymer arm MW was discovered to discourage star polymer formation, corroborating previous literature results. The relationship between polymer size in solution and polymer MW was determined for the linear and star polymers and the slight increases in size with star polymer MW verified previous theoretical results. This ability to synthesize arm-first star polymers from wedge ROMP polymers will facilitate the future development of polymeric materials with unique macroscopic behavior.

The self-assembly behavior of star polymers with block copolymer arms warrants further investigation. Previous work with linear wedge block copolymers indicates a limit of self-assembly in linear polymers with molecular weights above 1400 kDa. Implementing the star architecture with long polymer arms may improve the thermodynamics of self-assembly and create films which reflect wavelengths of light in the infrared band.

REFERENCES

(1) Vlassopoulos, D.; Fytas, G.; Pakula, T.; Roovers, J. Multiarm Star Polymers Dynamics. *J. Phys. Condens. Matter* **2001**, *13*, R855–R876 DOI: 10.1088/0953-8984/13/41/202.

(2) Roovers, J.; Zhou, L. L.; Toporowski, P. M.; Vanderzwan, M.; Iatrou, H.; Hadjichristidis, N. Regular Star Polymers With 64 and 128 Arms - Models for Polymeric Micelles. *J. Macromol.* **1993**, *26* (16), 4324–4331 DOI: 10.1021/ma00068a039.

(3) Morton, M.; Helminiak, T. E.; Gadkary, S. D.; Bueche, F. Preparation and Properties of Monodisperse Branched Polystyrene. *J. Polym. Sci.* **1962**, *57* (165), 471–482 DOI: 10.1002/pol.1962.1205716537.

(4) Ren, J. M.; McKenzie, T. G.; Fu, Q.; Wong, E. H. H.; Xu, J.; An, Z.; Shanmugam, S.; Davis, T. P.; Boyer, C.; Qiao, G. G. Star Polymers. *Chem. Rev.* **2016**, *116* (12), 6743–6836 DOI: 10.1021/acs.chemrev.6b00008.

(5) Lapienis, G. Star-Shaped Polymers Having PEO Arms. *Prog. Polym. Sci.* **2009**, *34* (9), 852–892 DOI: 10.1016/j.progpolymsci.2009.04.006.

(6) Gao, H. Development of Star Polymers as Unimolecular Containers for Nanomaterials. *Macromol. Rapid Commun.* **2012**, *33* (9), 722–734 DOI: 10.1002/marc.201200005.

(7) Wang, F.; Bronich, T. K.; Kabanov, A. V.; Rauh, R. D.; Roovers, J. Synthesis and Evaluation of a Star Amphiphilic Block Copolymer from Poly(ϵ-Caprolactone) and Poly(ethylene Glycol) as a Potential Drug Delivery Carrier. *Bioconjug. Chem.* **2005**, *16* (2), 397–405 DOI: 10.1021/bc049784m.

(8) Pang, X.; Zhao, L.; Han, W.; Xin, X.; Lin, Z. A General and Robust Strategy for the Synthesis of Nearly Monodisperse Colloidal Nanocrystals. *Nat. Nanotechnol.* **2013**, *8* (6), 426–431 DOI: 10.1038/nnano.2013.85.

(9) Xue, L.; Agarwal, U. S.; Lemstra, P. J. Shear Degradation Resistance of Star Polymers during Elongational Flow. *Macromolecules* **2005**, *38* (21), 8825–8832 DOI: 10.1021/ma0502811.

(10) Forman, D. C.; Wieberger, F.; Gröschel, A.; Müller, A. H. E.; Schmidt, H.-W.; Ober, C. K. Comparison of Star and Linear ArF Resists. **2010**, *7639*, 76390P DOI: 10.1117/12.848344.

(11) Yuan, W.; Yuan, J.; Zheng, S.; Hong, X. Synthesis, Characterization, and Controllable Drug Release of Dendritic Star-Block Copolymer by Ring-Opening Polymerization and Atom Transfer Radical Polymerization. *Polymer (Guildf).* **2007**, *48* (9), 2585–2594 DOI: 10.1016/j.polymer.2007.03.039.

(12) Ding, H.; Park, S.; Zhong, M.; Pan, X.; Pietrasik, J.; Bettinger, C. J.;

Matyjaszewski, K. Facile Arm-First Synthesis of Star Block Copolymers via ARGET ATRP with Ppm Amounts of Catalyst. *Macromolecules* **2016**, *49* (18), 6752–6760 DOI: 10.1021/acs.macromol.6b01597.

(13) Ren, J. M.; Fu, Q.; Blencowe, A.; Qiao, G. G. Organic Catalyst-Mediated Ring-Opening Polymerization for the Highly E Ffi Cient Synthesis of Polyester-Based Star Polymers. **2012**.

(14) Ooya, T.; Lee, J.; Park, K. Effects of Ethylene Glycol-Based Graft, Star-Shaped, and Dendritic Polymers on Solubilization and Controlled Release of Paclitaxel. *J. Control. Release* **2003**, *93* (2), 121–127 DOI: 10.1016/j.jconrel.2003.07.001.

(15) Qiu, Q.; Liu, G.; An, Z. Efficient and Versatile Synthesis of Star Polymers in Water and Their Use as Emulsifiers. *Chem. Commun.* **2011**, *47* (47), 12685 DOI: 10.1039/c1cc15679a.

(16) Altintas, O.; Yankul, B.; Hizal, G.; Tunca, U. A 3 -Type Star Polymers via Click Chemistry. *J. Polym. Sci. Part A Polym. Chem.* **2006**, No. July, 6458–6465 DOI: 10.1002/pola.

(17) Goh, T. K.; Coventry, K. D.; Blencowe, A.; Qiao, G. G. Rheology of Core Cross-Linked Star Polymers. *Polymer (Guildf).* **2008**, *49* (23), 5095–5104 DOI: 10.1016/j.polymer.2008.09.030.

(18) Likos, C. N.; Löwen, H.; Watzlawek, M.; Abbas, B.; Jucknischke, O.; Allgaier, J.; Richter, D. Star Polymers Viewed as Ultrasoft Colloidal Particles. *Phys. Rev. Lett.* **1998**, *80* (20), 4450–4453 DOI: 10.1103/PhysRevLett.80.4450.

(19) Watzlawek, M.; Likos, C. N.; Löwen, H. Phase Diagram of Star Polymer Solutions. *Phys. Rev. Lett.* **1999**, *82* (26), 5289–5292 DOI: 10.1103/PhysRevLett.82.5289.

(20) Matsushita, Y.; Hayashida, K.; Dotera, T.; Takano, A. Kaleidoscopic Morphologies from ABC Star-Shaped Terpolymers. *J. Phys. Condens. Matter* **2011**, *23* (28), 284111 DOI: 10.1088/0953-8984/23/28/284111.

(21) Rho, Y.; Kim, C.; Higashihara, T.; Jin, S.; Jung, J.; Shin, T. J.; Hirao, A.; Ree, M. Complex Self-Assembled Morphologies of Thin Films of an Asymmetric A 3B3C3 Star Polymer. *ACS Macro Lett.* **2013**, *2* (10), 849–855 DOI: 10.1021/mz400363k.

(22) Goseki, R.; Hirao, A.; Kakimoto, M. A.; Hayakawa, T. Cylindrical Nanostructure of Rigid-Rod POSS-Containing Polymethacrylate from a Star-Branched Block Copolymer. *ACS Macro Lett.* **2013**, *2* (7), 625–629 DOI: 10.1021/mz400125t.

(23) Jang, S.; Moon, H. C.; Kwak, J.; Bae, D.; Lee, Y.; Kim, J. K.; Lee, W. B. Phase Behavior of Star-Shaped Polystyrene-Block-Poly(methyl Methacrylate) Copolymers. *Macromolecules* **2014**, *47* (15), 5295–5302 DOI: 10.1021/ma500584x.

(24) Stenzel-Rosenbaum, M.; Davis, T. P.; Chen, V.; Fane, A. G. Star-Polymer

Synthesis via Radical Reversible Addition–fragmentation Chain-Transfer Polymerization. *J. Polym. Sci. Part A Polym. Chem.* **2001**, *39* (16), 2777–2783 DOI: 10.1002/pola.1256.

(25) Shibata, T.; Kanaoka, S.; Aoshima, S. Quantitative Synthesis of Star-Shaped Poly(vinyl Ether)s with a Narrow Molecular Weight Distribution by Living Cationic Polymerization. *J. Am. Chem. Soc.* **2006**, *128* (23), 7497–7504 DOI: 10.1021/ja057611h.

(26) Bellin, I.; Kelch, S.; Langer, R.; Lendlein, A. Polymeric Triple-Shape Materials. *Proc. Natl. Acad. Sci.* **2006**, *103* (48), 18043–18047 DOI: 10.1073/pnas.0608586103.

(27) Liu, J.; Burts, A. O.; Li, Y.; Zhukhovitskiy, A. V.; Ottaviani, M. F.; Turro, N. J.; Johnson, J. A. "Brush-First" method for the Parallel Synthesis of Photocleavable, Nitroxide-Labeled Poly(ethylene Glycol) Star Polymers. *J. Am. Chem. Soc.* **2012**, *134* (39), 16337–16344 DOI: 10.1021/ja3067176.

(28) Burts, A. O.; Gao, A. X.; Johnson, J. A. Brush-First Synthesis of Core-Photodegradable Miktoarm Star Polymers via ROMP: Towards Photoresponsive Self-Assemblies. *Macromol. Rapid Commun.* **2014**, *35* (2), 168–173 DOI: 10.1002/marc.201300618.

(29) Leitgeb, A.; Wappel, J.; Slugovc, C. The ROMP Toolbox Upgraded. *Polymer (Guildf).* **2010**, *51* (14), 2927–2946 DOI: 10.1016/j.polymer.2010.05.002.

(30) Miyake, G. M.; Weitekamp, R. A.; Piunova, V. A.; Grubbs, R. H. Synthesis of Isocyanate-Based Brush Block Copolymers and Their Rapid Self-Assembly to Infrared-Reflecting Photonic Crystals. *J. Am. Chem. Soc.* **2012**, *134* (34), 14249–14254 DOI: 10.1021/ja306430k.

(31) Piunova, V. A.; Miyake, G. M.; Daeffler, C. S.; Weitekamp, R. A.; Grubbs, R. H. Highly Ordered Dielectric Mirrors via the Self-Assembly of Dendronized Block Copolymers. *J. Am. Chem. Soc.* **2013**, *135* (41), 15609–15616 DOI: 10.1021/ja4081502.

(32) Boyle, B. M.; French, T. A.; Pearson, R. M.; McCarthy, B. G.; Miyake, G. M. Structural Color for Additive Manufacturing: 3D-Printed Photonic Crystals from Block Copolymers. *ACS Nano* **2017**, *11* (3), 3052–3058 DOI: 10.1021/acsnano.7b00032.

(33) Macfarlane, R. J.; Kim, B.; Lee, B.; Weitekamp, R. A.; Bates, C. M.; Lee, S. F.; Chang, A. B.; Delaney, K. T.; Fredrickson, G. H.; Atwater, H. A.; Grubbs, R. H. Improving Brush Polymer Infrared One-Dimensional Photonic Crystals via Linear Polymer Additives. *J. Am. Chem. Soc.* **2014**, *136* (50), 17374–17377 DOI: 10.1021/ja5093562.

(34) Hu, M.; Xia, Y.; Daeffler, C. S.; Wang, J.; McKenna, G. B.; Kornfield, J. A.; Grubbs, R. H. The Linear Rheological Responses of Wedge-Type Polymers. *J.*

Polym. Sci. Part B Polym. Phys. **2015**, *53* (13), 899–906 DOI: 10.1002/polb.23716.

(35) Li, Z.; Zhang, K.; Ma, J.; Cheng, C.; Wooley, K. L. Facile Syntheses of Cylindrical Molecular Brushes by a Sequential RAFT and ROMP “grafting-Through” methodology. *J. Polym. Sci. Part A Polym. Chem.* **2009**, *47* (20), 5557–5563 DOI: 10.1002/pola.23626.

(36) Hu, M.; Xia, Y.; McKenna, G. B.; Kornfield, J. A.; Grubbs, R. H. Linear Rheological Response of a Series of Densely Branched Brush Polymers. *Macromolecules* **2011**, *44* (17), 6935–6943 DOI: 10.1021/ma2009673.

(37) Rubin, S. F.; Kannan, R. M.; Kornfield, J. a.; Boeffel, C. Effect of Mesophase Order and Molecular Weight on the Dynamics of Nematic and Smectic Side-Group Liquid-Crystalline Polymers. *Macromolecules* **1995**, *28* (10), 3521–3530 DOI: 10.1021/ma00114a005.

(38) Fetters, L. J.; Lohse, D. J.; Graessley, W. W. Chain Dimensions and Entanglement Spacings in Dense Macromolecular Systems. *J. Polym. Sci. Part B Polym. Phys.* **1999**, *37* (10), 1023–1033 DOI: 10.1002/(SICI)1099-0488(19990515)37:10<1023::AID-POLB7>3.0.CO;2-T.

(39) Miyake, G. M.; Piunova, V. A.; Weitekamp, R. A.; Grubbs, R. H. Precisely Tunable Photonic Crystals From Rapidly Self-Assembling Brush Block Copolymer Blends. *Angew. Commun.* **2012**, *51* (45), 11246–11248 DOI: 10.1002/anie.201205743.

(40) Daoud, M.; Cotton, J. P. Star Shaped Polymers : A Model for the Conformation and Its Concentration Dependence. *J. Phys.* **1982**, *43* (3), 531–538 DOI: 10.1051/jphys:01982004303053100.

(41) Daoud, M.; Joanny, J. F. Conformation of Branched Polymers. *J. Phys.* **1981**, *42* (10), 1359–1371 DOI: 10.1051/jphys:0198100420100135900.

(42) Bauer, B. J.; Hadjichristidis, N.; Fetters, L. J.; Roovers, J. E. L. Star-Branched Polymers. 5. The Theta Temperature Depression for 8- and 12-Arm Polyisoprenes in Dioxane. *J. Am. Chem. Soc.* **1980**, *102*, 2410–2413 DOI: 10.1021/ja00527a045.

(43) Love, J. A.; Morgan, J. P.; Trnka, T. M.; Grubbs, R. H. A Practical and Highly Active Ruthenium-Based Catalyst That Effects the Cross Metathesis of Acrylonitrile. *Angew. Chemie - Int. Ed.* **2002**, *41* (21), 4035–4037 DOI: 10.1002/1521-3773(20021104)41.

(44) Wool, R. P. Polymer Entanglements. *Macromolecules* **1993**, *26* (7), 1564–1569 DOI: 10.1021/ma00059a012.